P9.3 RADIATIVE FLUX DIVERGENCE MEASUREMENTS DURING CASES-99

S. P. Burns*, J. Sun, A. C. Delany, S. P. Oncley, and T. W. Horst
National Center for Atmospheric Research, Boulder, Colorado

1. INTRODUCTION

The Cooperative Atmosphere-Surface Exchange Study (CASES-99) was a collaborate effort to study stable nocturnal boundary layers which took place during October, 1999 in the gently rolling hills east of Wichita, Kansas. Among an integrated set of tower, aircraft, and remote sensing measurements there was an array of 10 Eppley precision infrared radiometers, or pyrgeometers (model PIR) which measured the downwelling ($Q^{\downarrow}_{\rm LW}$) and upwelling ($Q^{\uparrow}_{\rm LW}$) longwave radiative fluxes at 48 m and 2 m. From these measurements the 2 components of the longwave flux divergence can be estimated.

The contribution of the vertical divergence of $Q_{\rm LW}$ to the thermal balance in a nocturnal, stable atmosphere has been measured in past experiments (Funk 1960; Nkemdirim 1978) but the interpretation of the results has been controversial and not in agreement with theory (Rider and Robinson 1951; Elliott 1964). Estimated vertical divergence of longwave radiation is presented in this paper.

2. MEASUREMENTS

The 10 PIRs used to measure the longwave fluxes are listed in Table 1 by serial number and location during deployment. In order to measure the vertical divergence of $Q_{\rm LW}$, 4 PIRs were mounted at the end of a 6 m boom about 48 m above the ground (2 upward and 2 downward looking), while the other 6 PIRs were mounted on 2 m radiation stands at 4 different ground stations s01, s02, s03, and s05 to estimate $Q^{\uparrow}_{\rm LW}$ and $Q^{\downarrow}_{\rm LW}$. The PIRs were all leveled and ventilated as described in Delany and Semmer (1998). At s01 and s02 there were both upward and downward looking PIRs while s03 and s05 only had downward looking PIRs. The maximum horizontal separation between any 2 PIRs was about 200 m and the station locations were chosen such that the dominant vegetation (short, medium, and tall pastureland grasses and plants of varying density) in the main tower area were sampled. For a more complete description of the experimental setup see the CASES-99 Operations Plan available on-line from the Colorado Research Associates (1999).

Serial No.	PIR location	s_e	B	c2	c1	c0	$Q^*_{\rm LW}$		$Q_{\rm LW}$
31976	48m	3.852	3.80	0.99	0.97	-0.39		↓	299.02
31980	48m	3.61	3.90	0.98	1.02	-2.45		↓	299.63
29260	s01	3.21	3.56	1.05	0.95	1.12	297.92	↓	292.19
31977	s02	3.729	3.50	0.98	0.97	-0.28	293.24	↓	292.97
31974	48m	3.854	3.95	(reference sensor)				↑	361.90
31978	48m	3.561	4.00	1.00	0.99	1.20		↑	361.96
26416	s01	3.57	3.56	1.04	0.78	1.48	355.80	↑	355.28
31981	s02	3.743	3.20	0.99	1.14	-0.13	353.74	↑	348.94
31975	s03	4.028	3.05	1.01	1.01	-0.57		↑	335.89
31979	s05	3.902	3.20	1.05	0.97	1.83		↑	356.27

Table 1: Calibration coefficients and 20-night mean values of nocturnal radiative fluxes for CASES-99 PIRs. $Q^*_{\rm LW}$ is the mean of the nighttime fluxes prior to applying the "ad-hoc" correction described in section 3.2. Units: s_e, μV/(W m^{-2}); $Q_{\rm LW}$ and c0, W m^{-2}; B, c1, and c2, dimensionless.

The Eppley PIR and calibration techniques are described by Fairall et al. (1998). The PIR $Q_{\rm LW}$ measurement is calculated by,

$$Q_{\rm LW} = {\rm c2}\frac{\Delta V}{s_e} + \sigma T_{\rm c}^4 - {\rm c1}B\sigma(T_{\rm d}^4 - T_{\rm c}^4) + {\rm c0}, \quad (1)$$

where ΔV is the thermopile voltage output; s_e is the Eppley radiometer sensitivity factor; σ is the Stefan-Boltzmann constant; $T_{\rm d}$ is the dome temperature; $T_{\rm c}$ is the case temperature; and B is the ratio of the dome emissivity to the transmissivity. The coefficients c0, c1, and c2 in Eq. (1) are determined from a field calibration (see section 3.1). Though analytic expressions exist for s_e and B, they are usually determined by calibration.

Prior to bringing the PIRs to Kansas all the case and dome thermistors (used to measure $T_{\rm c}$ and $T_{\rm d}$) were calibrated by the Atmospheric Technology Division (ATD) at the National Center for Atmospheric Research (NCAR) to within about ± 0.02°C of each other. The thermopiles were calibrated with a black body at the National Oceanic and Atmospheric Administration (NOAA) Environmental Research Laboratory (ERL) to determine s_e and B. The coefficients to convert the case and dome thermistor and thermopile voltages into physical quantities were manually entered into Campbell da-

* *Corresponding author address*: S. P. Burns, P.O. Box 3000, National Center for Atmospheric Research, Boulder, CO 80307-3000; e-mail: sean@ucar.edu.

ta loggers and then each data logger was assigned to a specific PIR. Since raw voltages were not recorded it was critical that each data logger stay with the PIR it was assigned (relevant to the correction described in section 3.2).

3. PIR DATA COMPARISONS

3.1 Side-by-Side Comparisons

During the 9 days prior to PIR deployment all 10 PIRs were set up side-by-side (0.11-0.35 m apart) on a single bench at the CASES-99 study site and $Q^{\downarrow}_{\rm LW}$ measurements from each PIR were compared. Assuming that the incoming longwave radiation incident upon each of the radiometers was identical, a least-squares minimization from 5 nights of $Q^{\downarrow}_{\rm LW}$ data was used to improve the relative accuracy of the PIR fluxes. The 5 nights of data used in the minimization were chosen based on weather conditions and whether all 10 PIRs were operating properly. To perform the optimization one PIR was chosen as the "reference" PIR (SN 31974) then c0, c1, and c2 were determined such that the difference between each PIR and the reference PIR was minimized. The resulting c0, c1, and c2 values for each PIR are listed in Table 1. PIR 31974 was picked as reference since its measurement of $Q^{\downarrow}_{\rm LW}$ was near the mean of $Q^{\downarrow}_{\rm LW}$ from all PIRs. The effect of optimizing the nocturnal data from the pre-CASES comparison period can be seen in Fig. 1 where the standard deviation of the differences is reduced from ± 0.9 W m^{-2} to ± 0.5 W m^{-2}. (During deployment, differences between the $Q_{\rm LW}$ nocturnal measurements were reduced by approximately the same amount as those shown in Fig. 1.) This technique improves the *relative* accuracy of the PIRs, but not necessarily the *absolute* accuracy.

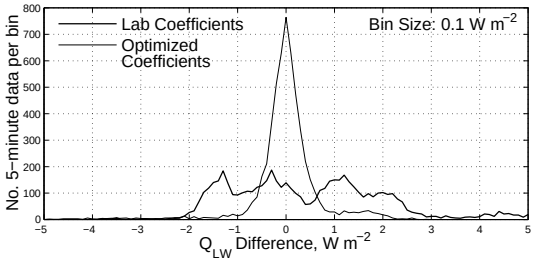

Figure 1: The frequency distribution of the difference between the reference PIR (SN 31974) and the other 9 PIRs. Data shown are 5-minute averages with (thin) and without (thick) optimization from 5 nights during the pre-CASES PIR comparison period.

3.2 Deployment Comparisons

On October 6, the PIRs were moved from their upward looking position on the comparison bench to the deployment locations (some PIRs were switched from upward looking to downward looking). Initial investigation of $Q^{\downarrow}_{\rm LW}$ nighttime data at s01 and s02 revealed differences of greater than 4 W m^{-2} as shown in the $Q^{*}_{\rm LW}$ column of Table 1. This difference seemed unreasonable since the PIRs at s01 and s02 were only separated by about 30 m and both were viewing the same nighttime sky. A similar evaluation of the $Q^{\uparrow}_{\rm LW}$ data cannot be done since s01 and s02 were over different types of vegetation and there was no expectation that these data should agree with each other. However, due to the large difference in $Q^{\downarrow}_{\rm LW}$ at s01 and s02, the data from all 4 PIRs at these stations were carefully scrutinized and it was discovered that the $T_{\rm c}$ and $T_{\rm d}$ data from both the upward and downward looking PIRs at s01 and s02 revealed some inconsistent features not seen in data from the other 6 PIRs. As an example, the $T_{\rm c}$ and $T_{\rm d}$ data from downward looking PIRs at s05 (SN 31979) and at s02 (SN 31981) are shown in Figs. 2a and 2b, respectively.

When the instruments were moved there was a mix-up of data loggers and PIRs at s01 and s02 (the PIRs which were supposed to go to s01 went to s02 and vice versa). After the mix-up was discovered, it was decided to modify the coefficients in the data loggers at s01 and s02 rather than do the labor-intensive task of moving the PIRs. The coefficients were modified on October 8, which is indicated by

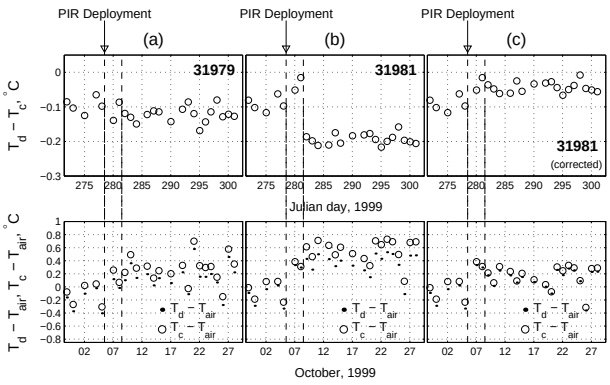

Figure 2: Nighttime 10-hour mean temperatures differences between the PIR case $T_{\rm c}$ and dome $T_{\rm d}$ (upper panels) and $T_{\rm c}$ and $T_{\rm d}$ compared with the average air temperature $T_{\rm air}$ from the 6 ground stations (lower panels). Differences between these temperatures are compared for PIR (a) SN 31979, (b) SN 31981, and (c) SN 31981 with "ad hoc" corrections to $T_{\rm c}$ and $T_{\rm d}$ data. The first vertical line indicates when the PIRs were moved from the pre-CASES comparison location to the stations for deployment. The second vertical line indicates when data-logger coefficients were changed by ATD personnel for PIR 31981. Tick marks are at 0:0:0 CDT in both upper and lower panels.

the second vertical line in the panels of Fig. 2. It should be noted that the PIR 31981 data between October 6 and 8 shown in Figs. 2b and 2c were corrected in post-processing for the PIR mix-up. Assuming the characteristics of T_c and T_d should be similar to what was seen between October 6th and 8th, it was deemed necessary to determine "ad-hoc" corrections to the T_c and T_d data for the PIRs at s01 and s02. The ad-hoc corrections were determined based on two factors: (1) comparing the absolute value of T_c and T_d to an estimate of the nighttime ambient air temperature T_{air} (calculated by averaging the air temperature at the 6 stations) from the night of October 16th (further explained below), and (2) maintaining a consistent T_d and T_c difference with what was observed during the nights of October 6th and 7th. Data from the night of October 16th were used to determine the absolute value of these corrections because the atmosphere was vertically and horizontally well mixed (wind speed was around 9 m s^{-1}, and the 2.5-hour mean air temperature differences between the ground stations were extremely small (less than $\pm 0.1°C$)). For this particular night, T_c and T_d from the PIRs at 48m, s03 and s05 showed close agreement with T_{air}, but T_c and T_d from the PIRs at s01 and s02 were greater than T_{air} by 0.3-0.6°C. From these data the ad-hoc corrections were determined and are listed in Table 2 (also, see Fig. 2c). The thermopile output from these PIRs appeared similar before and after the data logger coefficients were changed (not shown here), so the ad-hoc correction was only applied to T_c and T_d data.

Downwelling longwave radiative fluxes calculated with the ad-hoc corrected T_c and T_d data results in improved agreement between s01 and s02 $Q^{\downarrow}_{LW}$ measurements. The difference in the 20-day mean nocturnal downwelling flux between s01 and s02 is reduced from 4 W m^{-2} to less than 1 W m^{-2}, as shown in Table 1.

4. RESULTS

The measured longwave radiative fluxes at each station from the 20 days of deployment are com-

	Upward Looking		Downward Looking	
	29260 s01	31977 s02	26416 s01	31981 s02
T_c	-0.4	-0.4	-0.4	-0.4
T_d	-0.2	-0.5	-0.5	-0.25

Table 2: Ad-hoc corrections applied to the s01 and s02 PIRs case T_c and dome T_d temperatures. All values in degrees Celsius.

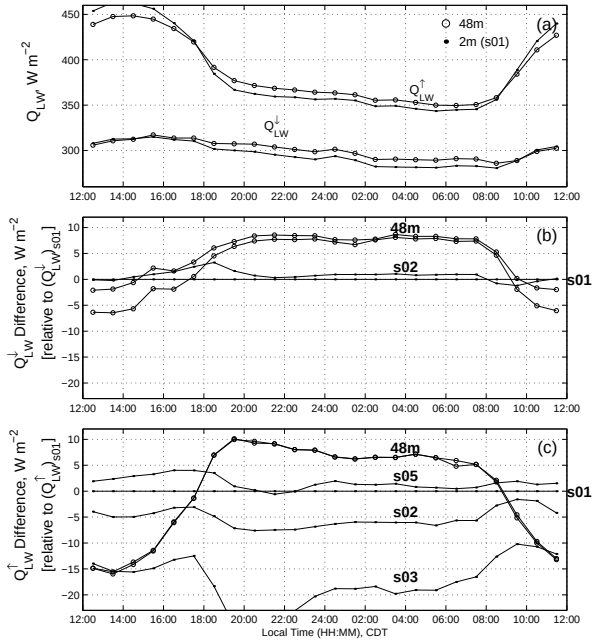

Figure 3: Hourly bin-averaged measurements for the entire 20 day deployment time period of (a) $Q^{\downarrow}_{LW}$ and $Q^{\uparrow}_{LW}$ from 48m and from s01, (b) the difference between $Q^{\downarrow}_{LW}$ at s01 and at the other stations, and (c) the difference between $Q^{\uparrow}_{LW}$ at s01 and at other stations.

posited in Fig. 3. For the ground station data, $Q^{\downarrow}_{LW}$ data at s01 and s02 were found to be in closer agreement at night because no correction for solar heating was used and the optimization method used only nighttime data. $Q^{\uparrow}_{LW}$ revealed significant differences depending upon the type of vegetation beneath the PIR as well as the prevailing environmental conditions at that particular station.

The s03 PIR was above tall, dense grass and in a low-elevation location which was subject to cold-air drainage flows at night. (The nocturnal air temperature at s03 was, on average, 1°C colder than s01 and 0.5°C colder than s02 and s05.) The s02 PIR was over spotty patches of medium length grass which was between the length of the s03 grass and that at s01 and s05 (where there was short grass and exposed ground). A surface survey with a hand-held infrared radiometer showed that the surface radiative temperature decreases as the grass density and height increases. This is consistent with what is observed in the $Q^{\uparrow}_{LW}$ data (Fig 3c). Conditions at the study site during the month of October were extremely dry (only a trace of rain) and generally cloud-free.

Based on field notes and photos taken from the

top of the tower, the area surrounding the tower is simplified into several surface types from which we have $Q^{\uparrow}_{\rm LW}$ measurements. By keeping the same observational view as the PIRs at 48 m, $Q^{\uparrow}_{\rm LW}$ at 2 m can be formulated as,

$$(Q^{\uparrow}_{\rm LW})_{\rm 2m} = 0.965(Q^{\uparrow}_{\rm LW})_{\rm s01} + 0.018(Q^{\uparrow}_{\rm LW})_{\rm s02} + 0.017(Q^{\uparrow}_{\rm LW})_{\rm s03}, \quad (2)$$

where the weights for each station are calculated by integrating the contribution from each surface type to $Q^{\uparrow}_{\rm LW}$ at 48 m. The downwelling flux measured at 2 m $(Q^{\downarrow}_{\rm LW})_{\rm 2m}$ was estimated by averaging the data from s01 and s02. At 48 m the upwelling and downwelling fluxes are averages of the PIR measurements made there. With Eq. (2), and assuming constant air density and specific heat, an estimate of the cooling rate due to net longwave flux divergence of the air column between 2 and 48 m can be estimated and compared with the measured atmospheric cooling rate from several different levels on the main tower (Fig. 4).

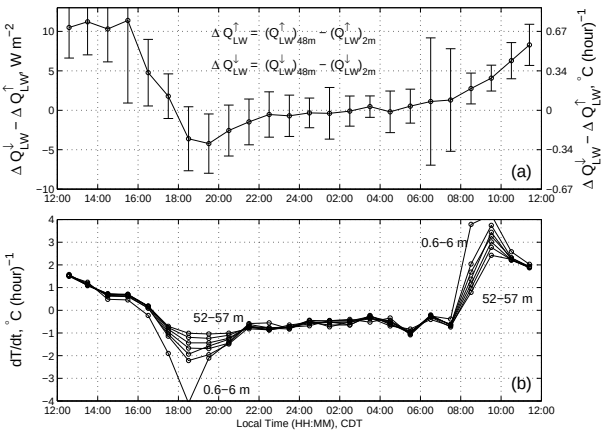

Figure 4: Hourly bin-averaged measurements for the entire 20 day deployment time period of (a) the net radiative flux divergence and (b) the average cooling rate at 6 levels from the main tower thermocouple data. The error bars in Fig. 4a indicate plus-or-minus one standard deviation of the data in that bin.

5. CONCLUSIONS

Radiative longwave flux measurements were made during CASES-99 with PIRs at 48 m and 2 m to produce an estimate of the net longwave radiative flux divergence. Data from a pre-CASES quality check with all 10 PIRs looking upward and situated very close to each other were used to reduce the relative error between the PIRs from ± 0.9 W m^{-2} to ± 0.5 W m^{-2} (nighttime data only).

On average, the net longwave radiative flux was found to be significant from sunset till just before midnight after which time it produced very little cooling of the atmosphere. The period of maximum longwave radiative cooling and maximum bulk atmospheric cooling both occur just after sunset with magnitudes of about -0.3°C hr^{-1} and -1.5°C hr^{-1}, respectively (Fig. 4). Whereas the results given here are an ensemble of the longwave radiation measurements during CASES-99, it should be noted that several nights revealed a maximum longwave radiative cooling rate of over -0.7°C hr^{-1}.

6. ACKNOWLEDGEMENTS

We acknowledge all NCAR ATD personnel who helped with the calibration, deployment, and maintenance of the CASES-99 PIRs. We also thank Ellsworth Dutton of NOAA/ERL for overseeing the PIR calibrations. This work was supported by Army Research Office Grant DAAD1999-1-0320 and National Science Foundation Grant ATM-9906637.

7. REFERENCES

Colorado Research Associates (CoRA), cited 1999: Cooperative Atmospheric Surface Exchange Study 1999, operations plan, 1-31 October 1999. [Available on-line from http://www.colorado-research.com/cases/CASES-99.html.]

Delany, A. C., and S. R. Semmer, 1998: An integrated surface radiation measurement system. *J. Atmos. Oceanic Technol.*, **15**, 46-53.

Elliot, W. P., 1964: The height variation of vertical heat flux near the ground. *Quart. J. Roy. Met. Soc.*, **90**, 260-265.

Fairall, C. W., et al., 1998: A new look at calibration and use of Eppley Precision Infrared Radiometers. Part I: Theory and application. *J. Atmos. Oceanic Technol.*, **15**, 1229-1242.

Funk, J. P., 1960: Measured radiative flux divergence near the ground at night. *Quart. J. Roy. Met. Soc.*, **86**, 382-389.

Nkemdirim, L. C., 1978: A comparison of radiative and actual nocturnal cooling rates over grass and snow. *J. Appl. Meteor.*, **17**, 1643-1646.

Rider, N. E., and G. D. Robinson, 1951: A study of the transfer of heat and water vapour about a short grass surface. *Quart. J. Roy. Met. Soc.*, **77**, 375-401.